

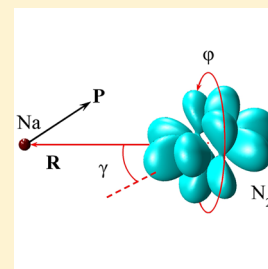
# Accurate Calculations of Rotationally Inelastic Scattering Cross Sections Using Mixed Quantum/Classical Theory

Alexander Semenov and Dmitri Babikov\*

Chemistry Department, Wehr Chemistry Building, Marquette University, Milwaukee, Wisconsin 53201-1881, United States

**ABSTRACT:** For computational treatment of rotationally inelastic scattering of molecules, we propose to use the mixed quantum/classical theory, MQCT. The old idea of treating translational motion classically, while quantum mechanics is used for rotational degrees of freedom, is developed to the new level and is applied to Na + N<sub>2</sub> collisions in a broad range of energies. Comparison with full-quantum calculations shows that MQCT accurately reproduces all, even minor, features of energy dependence of cross sections, except scattering resonances at very low energies. The remarkable success of MQCT opens up wide opportunities for computational predictions of inelastic scattering cross sections at higher temperatures and/or for polyatomic molecules and heavier quenchers, which is computationally close to impossible within the full-quantum framework.

**SECTION:** Kinetics and Dynamics



Inelastic scattering processes play important roles in a broad variety of chemical and physical phenomena. For example, they are crucial for quantitative interpretation of molecular spectra observed in astrochemical environments,<sup>1</sup> modeling atmospheric chemistry,<sup>2,3</sup> development of cooling and trapping techniques at ultracold temperatures,<sup>4,5</sup> and description of thermalization of enthalpy released by chemical bonds in combustion.<sup>6,7</sup> Calculations of inelastic cross sections are usually carried out using quantum scattering codes such as MOLSCAT, but the full-quantum scattering calculations, physically indispensable and computationally affordable at low temperatures,<sup>8</sup> become prohibitively demanding at higher temperatures and/or for heavier (polyatomic) molecules and quenchers.<sup>9</sup> It is important to realize that at such conditions, the intermolecular degrees of freedom can be treated classically. Computationally powerful and physically appropriate methods for description of inelastic scattering can be formulated if the classical trajectory treatment of scattering is interfaced with quantum treatment of rotation (and/or vibration) in a self-consistent way, which allows energy exchange between external and internal degrees of freedom but keeps total energy conserved. Such a method is not expected to handle purely quantum phenomena in the translational motion, such as shape resonances and scattering at sub-Kelvin temperatures (when the de Broglie wavelength becomes comparable to the interaction range), but it may be rather accurate at higher temperatures, when quantum phenomena are less important.

The idea of such mixed quantum/classical theory (MQCT) is not entirely new, but it has never been fully developed to the level of a predictive computational tool. Foundations of this theory have been outlined by Gert Billing and applied to one (relatively simple) system, He + H<sub>2</sub>, at two (relatively high) values of scattering energies,  $E = 0.1$  and  $0.9$  eV.<sup>10,11</sup> Those ground-breaking results were included in the review paper<sup>12</sup> and the book<sup>13</sup> but, surprisingly, remained the only example of MQCT treatment of rotationally inelastic scattering. Knowing

about the success of the mean-field methods for electronic structure calculations (such as Hartree–Fock and DFT), it is almost astonishing to find out that a similar approach has not been pursued in the quantum dynamics simulations of nuclear motion.

Careful analysis of Billing's work reveals that he employed only an approximate version of MQCT, known as the coupled states (CS) approximation, where transitions between different  $m$  states, within the same rotational energy level  $j$ , are entirely neglected. Also, the equations Billing used assume a simplified sampling procedure;<sup>12,13</sup> they cannot be used to handle a general case. In a recent theory paper,<sup>14</sup> we presented and tested, using a model system, the general and fully coupled version of MQCT, formulated in both laboratory-fixed and body-fixed (BF) reference frames. In this Letter, we report results of first application of the fully coupled MQCT to a real system, Na + N<sub>2</sub>, for which the full-quantum data are available in a broad range of collision energies<sup>15</sup> and a detailed comparison of results is straightforward.

In the BF reference frame (see the Table of Contents figure), the rotational and vibrational motion of a diatomic molecule is described by coordinates  $\mathbf{q} = (r, \gamma, \varphi')$ . These are quantum degrees of freedom; their evolution is determined by the wave function  $\psi(r, \gamma, \varphi')$ . The scattering of the quencher atom, here Na, is described by spherical polar coordinates  $\mathbf{Q} = (R, \Theta, \Phi)$ . These are classical degrees of freedom; their evolution is determined by conjugate momenta  $P_R$ ,  $P_\Theta$ , and  $P_\Phi$ . The interaction potential does not depend on classical angles and the angle  $\varphi'$  due to symmetry; therefore,  $V = V(R, r, \gamma)$ . The MQCT equations of motion for classical variables, obtained in ref 14, are

**Received:** November 22, 2013

**Accepted:** December 26, 2013

$$\dot{R} = \frac{P_R}{\mu} \quad (1)$$

$$\dot{\Theta} = \frac{P_\Theta}{\mu R^2} \quad (2)$$

$$\dot{\Phi} = \frac{P_\Phi}{\mu R^2 \sin^2 \Theta} \quad (3)$$

$$\dot{P}_R = -\frac{\partial \tilde{V}(R)}{\partial R} + \frac{P_\Theta^2}{\mu R^3} + \frac{P_\Phi^2}{\mu R^3 \sin^2 \Theta} \quad (4)$$

$$\begin{aligned} \dot{P}_\Theta = & \sum_{n''j''m''} \sum_{n'j'm'} a_{n''j''m''}^* a_{n'j'm'} \exp\{i(E_{n''j''} - E_{n'j'})t/\hbar\} \\ & \times [\mathbf{M}, \mathbf{U}]_{n'j'm'}^{n''j''m''} + \frac{P_\Phi^2 \cos \Theta}{\mu R^2 \sin^3 \Theta} \end{aligned} \quad (5)$$

$$\begin{aligned} \dot{P}_\Phi = & -i \sum_{n''j''m''} \sum_{n'j'm'} a_{n''j''m''}^* a_{n'j'm'} \exp\{i(E_{n''j''} - E_{n'j'})t/\hbar\} \\ & \sin \Theta [\mathbf{M}, \mathbf{V}]_{n'j'm'}^{n''j''m''} \end{aligned} \quad (6)$$

Here, we introduced the mean-field potential  $\tilde{V}(R) = \langle \psi(r, \gamma, \varphi') | V(R, r, \gamma) | \psi(r, \gamma, \varphi') \rangle$  and the commutators  $[\mathbf{M}, \mathbf{U}]$  and  $[\mathbf{M}, \mathbf{V}]$  of matrices discussed below. Expansion of wave function over the basis set of rovibrational eigenstates with time-dependent coefficients  $a_{njm'}(t)$  and substitution into the Schrodinger equation leads to

$$\begin{aligned} i\hbar \frac{\partial a_{njm'}}{\partial t} = & \sum_{n'j'} a_{n'j'm'} \exp\{i(E_{nj} - E_{n'j'})t/\hbar\} M_{nj'}^{n'j'}(R) \\ & - i\hbar \sum_{m''} a_{njm''} W_{m''}^{m'} \end{aligned} \quad (7)$$

The structure of these coupled equations is such that the state-to-state transition matrix  $M_{nj'}^{n'j'}$ , introduced for every  $m'$  as

$$M_{nj'}^{n'j'}(R) = A_{j'm'jm'} \langle \varphi_{nj}(r) P_{jm'}(\cos \gamma) | V(R, r, \gamma) | \varphi_{n'j'}(r) P_{j'm'}(\cos \gamma) \rangle \quad (8)$$

describes only transitions from  $(nj)$  to  $(n'j')$ , within the same value of  $m'$  (coefficients  $A_{j'm'jm'}$  originate from normalization; see ref 14). In contrast, the matrix  $W_{m''}^{m'}$ , introduced for every  $j$ , describes transitions between  $m'$  and  $m'' = m' \pm 1$ , within the same energy level  $(nj)$ . Its elements are expressed as

$$W_{m''}^{m'} = U_{m''}^{m'} \dot{\Theta} + i(\sin \Theta V_{m''}^{m'} - m'' \cos \Theta \delta_{m', m''}) \dot{\Phi} \quad (9)$$

through elements of two simpler matrixes<sup>14</sup>

$$\begin{aligned} U_{m''}^{m'} = & \frac{1}{2} [\sqrt{j(j+1) - m''(m''-1)} \delta_{m', m''-1} \\ & - \sqrt{j(j+1) - m''(m''+1)} \delta_{m', m''+1}] \end{aligned} \quad (10)$$

and

$$\begin{aligned} V_{m''}^{m'} = & \frac{1}{2} [\sqrt{j(j+1) - m''(m''-1)} \delta_{m', m''-1} \\ & + \sqrt{j(j+1) - m''(m''+1)} \delta_{m', m''+1}] \end{aligned} \quad (11)$$

Matrixes  $\mathbf{M}$ ,  $\mathbf{U}$ , and  $\mathbf{V}$  are real-valued, sparse, and time-independent (should be computed only once). Note that elements of matrix  $\mathbf{M}$  and the mean-field potential  $\tilde{V}$  depend on  $R$  only. The values of each matrix element were precomputed

on a grid of 400 points along  $R$ , and a spline of these data was employed to supply the values of matrix elements and their derivatives at arbitrary  $R$  as classical trajectories were propagated through the interaction region. Note that the interaction potential is exact with all couplings included, and no terms in the kinetic energy operator are neglected (no decoupling approximation of any sort).

We used the same potential energy surface as that in the full-quantum calculations of ref 15, expanded in terms of Legendre polynomials,  $V(R, \gamma) = \sum V_n(R) P_n(\cos \gamma)$ . For the Na + N<sub>2</sub>( $\nu=0$ ) system, we included all even terms up to  $n=8$  and used the  $R$ -dependent expansion coefficients  $V_n(R)$  from ref 15. Vibrational motion was held frozen, and the transition matrix elements in eq 8 were averaged over wave function of the ground vibrational state. Equations 1–7 were numerically solved altogether using the Runge–Kutta method of fourth order. The initial molecule–quencher separation was close to  $R = 28 a_0$ . The classical impact parameter was sampled randomly using the Monte Carlo technique in the range from 0 to  $b_{\max} = 24 a_0$ , determined by convergence studies. The magnitude of the classical momentum is chosen as prescribed by the symmetrized average velocity approach,<sup>16</sup> which takes into account microscopic reversibility of state-to-state transitions. The probability amplitudes at the final moment of time  $a_{j'm'}(t = +\infty)$  are used to compute cross sections for transitions from initial  $j_{\text{ini}}$  to final  $j_{\text{fin}}$  rotational levels

$$\sigma = \frac{1}{(2j_{\text{ini}} + 1)} \sum_{m'} \frac{\pi}{k^2} \frac{J_{\max}}{N} \sum_i (2J^{(i)} + 1) \sum_{m''} |a_{j_{\text{fin}} m''}^{(i)}|^2 \quad (12)$$

In this formula, transition probabilities are first summed over the final values  $-j_{\text{fin}} \leq m'' \leq +j_{\text{fin}}$ , then averaged over  $N$  classical trajectories labeled by  $i$  (typically, a few hundred randomly sampled values of the impact parameter), and finally, averaged over the initial values  $-j_{\text{ini}} \leq m' \leq +j_{\text{ini}}$ . Note that  $J_{\max} = k\hbar b_{\max}$ .

In Figure 1, we compare cross sections computed using MQCT against the full-quantum results from ref 15 for

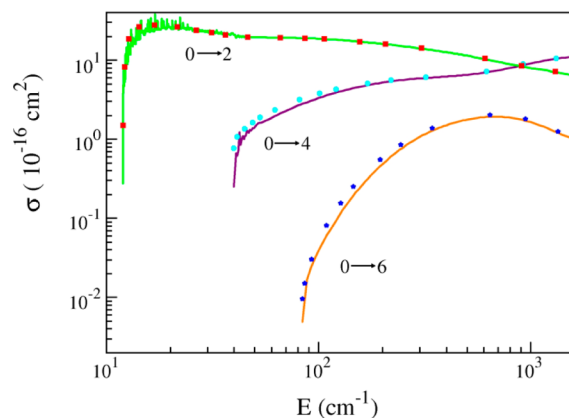


**Figure 1.** Inelastic scattering cross section for transitions from  $j = 0$  to 2, 4, and 6. Full-quantum results from ref 15 are shown by lines. Our MQCT results are shown by symbols.

excitation of the ground rotational state  $j_{\text{ini}} = 0$  at different collision energies. For homonuclear N<sub>2</sub> in  $j_{\text{ini}} = 0$ , the allowed transitions are  $0 \rightarrow 2$ ,  $0 \rightarrow 4$ ,  $0 \rightarrow 6$ , and so forth, and we see that all three  $\sigma(E)$  dependencies are accurately reproduced in a broad range of energies,  $12 \leq E \leq 1500 \text{ cm}^{-1}$ , and through a four orders of magnitude range of  $\sigma$  values. As energy  $E$

increases, the value of  $\sigma$  for  $0 \rightarrow 2$  decreases, while it increases for  $0 \rightarrow 4$ , and it passes through a maximum for the  $0 \rightarrow 6$  transition. All of these features are reproduced by MQCT. Even details of  $\sigma(E)$  dependencies, such as slight deviations from the monotonic behavior (i.e., small oscillations), are also reproduced. The channel thresholds are correctly predicted.

The process  $0 \rightarrow 2$ , which has the smallest value of energy quantum,  $\Delta E = 11.9 \text{ cm}^{-1}$ , is reproduced by MQCT particularly well. Some (relatively small) errors are observed for transitions  $0 \rightarrow 4$  and  $0 \rightarrow 6$ , where the quantum of energy increases to  $\Delta E = 39.8$  and  $83.5 \text{ cm}^{-1}$ , respectively. This is understood because the MQCT is not expected to be particularly accurate at the channel threshold, when the collision energy  $E$  is comparable to the quantum of excitation  $\Delta E$ . Also, resonances at small energies (clearly present in the case of  $0 \rightarrow 2$ ; see Figure 1) are not expected to be reproduced by MQCT. Thus, we restricted our analysis to nonresonant cross sections only and simply zeroed all trajectories that exhibited resonant behavior. At collision energies  $E > 2\Delta E$ , the deviation of MQCT cross sections from full-quantum results is only a few percent.

Figure 2 shows computed  $\sigma(E)$  dependencies for the excited rotational state  $j_{\text{ini}} = 5$ . In this case, the allowed excitation

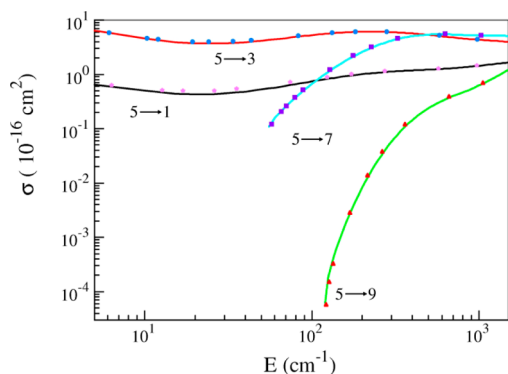


**Figure 2.** Same as Figure 1 but for transitions from  $j = 5$  to 1, 3, 7, and 9.

processes are  $5 \rightarrow 7$ ,  $5 \rightarrow 9$ , and so forth, while the allowed quenching processes are  $5 \rightarrow 3$  and  $5 \rightarrow 1$ . In all cases, MQCT reproduced quantum results accurately. Note that for quenching processes, excellent agreement is observed down to  $E = 5 \text{ cm}^{-1}$ , and even small oscillations of  $\sigma(E)$  are reproduced.

We also found that MQCT permits one to compute the scattering phase and obtain, using standard quantum expressions, the differential (over the scattering angle) cross section, including that for the elastic channel. It is well-known that neither the elastic nor the differential cross section can be reproduced by the classical scattering theory due to the lack of phase information and quantum interference. However, MQCT has all of that. Figure 3 shows quantum oscillations of the differential cross section for the elastic scattering channel  $0 \rightarrow 0$  at collision energy  $E = 50 \text{ cm}^{-1}$ . Again, every oscillation of the quantum result<sup>15</sup> is reproduced by MQCT including the vicinity of the rainbow angle and even at small scattering angles, where the semiclassical approximation is usually not expected to be accurate.

Classical treatment of scattering is justified if the de Broglie wavelength is small, compared to the effective range of interaction,  $(\lambda/a)^{1/2} \ll 1$ . In the  $\text{N}_2 + \text{Na}$  system studied

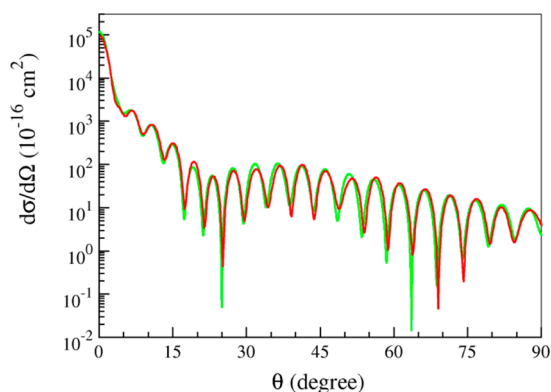


**Figure 3.** Differential scattering cross section for the elastic channel  $j = 5$  at collision energy  $E = 50 \text{ cm}^{-1}$ . Full-quantum results from ref 15 are shown by the green line, and our MQCT results are shown by the red line. The rainbow angle is at  $67.5^\circ$ .

here, the well depth of the PES is close to  $24 \text{ cm}^{-1}$ , with the minimum point located at the distance of roughly  $11 a_0$ . The condition  $\tilde{\lambda} = a$  is approximately satisfied at a collision energy of  $E = 1.7 \text{ cm}^{-1}$ . Thus, one can safely say that all results of this Letter are unaffected by the de Broglie condition for translational motion.

In order to obtain a better practical measure of MQCT accuracy, we computed total rate coefficients for inelastic scattering from  $j = 0$  at three temperatures,  $T = 100, 205,$  and  $300 \text{ K}$ , and compared our data with full-quantum results of ref 15,  $\kappa = 8.80, 12.1,$  and  $14.5 \times 10^{-11} \text{ cm}^3 \text{ s}^{-1}$ , respectively. We found that the rate coefficients predicted by MQCT were different by only +1.5, +1.0, and +0.6%, respectively.

The CS approximation, within MQCT, is easily formulated by neglecting the last term in eq 7 and simplifying eqs 5 and 6 accordingly.<sup>14</sup> Such a simplified version of MQCT was used by Billing in the past.<sup>10,11</sup> We also tested this method and found that results of CS-MQCT follow the full-quantum results qualitatively but not quantitatively. Details of  $\sigma(E)$  dependencies, such as oscillations of cross sections, are not reproduced correctly. Often, large errors are found. For example, at  $E = 120 \text{ cm}^{-1}$ , the value of  $\sigma$  for  $0 \rightarrow 2$  is smaller by 25% compared to the full-quantum result (while the fully coupled MQCT is off by less than 0.5%; see Figure 1). Errors of CS-MQCT are even larger near channel thresholds. For example, the value of  $\sigma$  for  $5 \rightarrow 9$  at  $E = 120 \text{ cm}^{-1}$  is underestimated by 62% compared to the full-quantum result. In contrast, the fully coupled MQCT works reasonably well even near threshold (only  $\sim 5\%$  deviation; see Figure 2).

We have also run the purely classical trajectories for this process and tried various known methods of the final state analysis,<sup>17</sup> but, when applied to all various state-to-state cross sections, neither method worked consistently better than others. Furthermore, because  $\text{N}_2$  is symmetric, one should introduce an ad hoc factor of  $\times 1/2$  (which would be hard to justify in the case of different isotopes). Only then do the results of classical trajectories fall into the right order of magnitude range, and some, but not all,  $\sigma(E)$  dependencies are reproduced (qualitatively but not quantitatively). Some of the classical state-to-state cross sections are higher, while others are lower compared to quantum results, typically by a factor of 2–4. Near the channel threshold for excitation (and at lower collision energy for quenching), the classical cross section is underestimated, typically by 2 orders of magnitude.

In contrast, the level of agreement between MQCT and full-quantum calculations is very encouraging, if not to say exciting. We want to stress that MQCT was applied without any adjustments, according to eqs 1–12 and the symmetrized average velocity approach,<sup>17</sup> which makes this general theory an excellent candidate for the “black box” utilization in a broad spectrum of applications,<sup>1–3,6,7,10</sup> even by nonexpert users. The computer code is simple, and calculations are highly affordable (here,  $\sim 1$  min on a single processor per energy point). Furthermore, calculations with different impact parameters are entirely independent, which makes this method intrinsically parallel; one can easily spread MQCT trajectories onto hundreds of processors with zero communication overlap.

The focus of this Letter is on rotational transitions, but in a recent paper,<sup>17</sup> we reported a successful application of MQCT to vibrational quenching in CO + He collisions. Combined, these two studies open new opportunities for efficient theoretical treatment of general inelastic rovibrational processes. The results obtained so far indicate that MQCT is more accurate for heavier masses, at higher collision energies and smaller spacings between quantized states (energy quanta). Importantly, in this regime, the full-quantum method becomes computationally costly, while the MQCT calculations become very affordable. Namely, we found that at higher energies, the number of MQCT trajectories needed for convergence is smaller, and the numerical effort to propagate each trajectory through the interaction region is lower. The reduced mass of collision partners does not affect significantly the cost of MQCT calculations, making it affordable even for polyatomic molecules. As for energy quanta, the low-lying states (considered here for rotational and in ref 16 for vibrational transitions) represent the most stringent test of the method. Closer to the dissociation limit, where the quanta are smaller and the system is more classical,<sup>16</sup> MQCT is expected to be very accurate. It is true that a large density of accessible rovibrational states (e.g., near the dissociation limit or in a polyatomic molecule) will increase significantly the size of matrix  $M$  in eq 8, but exactly the same issue is encountered in the full-quantum calculations, and it is usually not a problem to compute the state-to-state transition matrix  $M$ . The bottleneck of the full-quantum method is to propagate the system of coupled equations for scattering, which is avoided in the MQCT where it is replaced by propagation of independent classical trajectories, eqs 1–6. Overall, MQCT seems to be an attractive alternative to the standard full-quantum approach, particularly at higher energies, for heavier masses, and when the internal quanta are small.

## AUTHOR INFORMATION

### Corresponding Author

\*E-mail: dmitri.babikov@mu.edu.

### Notes

The authors declare no competing financial interest.

## ACKNOWLEDGMENTS

This research was supported by NSF, partially through the Atmospheric Chemistry Program, Grant #1252486, and partially through the Theoretical Chemistry Program, Grant #1012075. This research used resources of the National Energy Research Scientific Computing Center, which is supported by the Office of Science of the U.S. Department of Energy under Contract No. DE-AC02-05CH11231.

## REFERENCES

- (1) Daniel, F.; Dubernet, M.-L.; Pacaud, F.; Grosjean, A. Rotational Excitation of 20 Levels of Para-H<sub>2</sub>O by Ortho-H<sub>2</sub> ( $j_2 = 1, 3, 5, 7$ ) at High Temperature. *Astron. Astrophys.* **2010**, *A13*, 517–523.
- (2) Ivanov, M. V.; Babikov, D. Efficient Quantum-Classical Method for Computing Thermal Rate Constant of Recombination: Application to Ozone Formation. *J. Chem. Phys.* **2012**, *136*, 184304/1–184304/16.
- (3) Ivanov, M. V.; Babikov, D. On Molecular Origin of Mass-Independent Fractionation of Oxygen Isotopes in the Ozone Forming Recombination Reaction. *Proc. Natl. Acad. Sci. U.S.A.* **2013**, *110*, 17708/1–17708/5.
- (4) Balakrishnan, N.; Dalgarno, A.; Forrey, R. C. Vibrational Relaxation of CO by Collisions With <sup>4</sup>He at Ultracold Temperatures. *J. Chem. Phys.* **2000**, *113*, 621–627.
- (5) Balakrishnan, N.; Forrey, R. C.; Dalgarno, A. Complex Scattering Lengths in Multi-Channel Atom–Molecule Collisions. *Chem. Phys. Lett.* **1997**, *280*, 5–9.
- (6) Sevy, E. T.; Rubin, S. M.; Lin, Z.; Flynn, G. W. Translational and Rotational Excitation of the CO<sub>2</sub>(00<sup>0</sup>) Vibrationless State in the Collisional Quenching of Highly Vibrationally Excited 2-Methylpyrazine: Kinetics and Dynamics of Large Energy Transfers. *J. Chem. Phys.* **2000**, *113*, 4912–4932.
- (7) Barker, J. R.; Weston, R. E., Jr. Collisional Energy Transfer Probability Densities  $P(E, J; E', J')$  for Monatomics Colliding with Large Molecules. *J. Phys. Chem. A* **2010**, *114*, 10619–10633.
- (8) Cecchi-Pestellini, C.; Bodo, E.; Balakrishnan, N.; Dalgarno, A. Rotational and Vibrational Excitation of CO Molecules by Collisions with <sup>4</sup>He Atoms. *Astrophys. J.* **2002**, *571*, 1015–1020.
- (9) Wiesenfeld, L.; Scribano, Y.; Faure, A. Rotational Quenching of Monodeuterated Water by Hydrogen Molecules. *Phys. Chem. Chem. Phys.* **2011**, *13*, 8230–8235.
- (10) Billing, G. D. The Semiclassical Coupled States Method. *J. Chem. Phys.* **1976**, *65*, 1–6.
- (11) Billing, G. D. Comparison of Quantum Mechanical and Semiclassical Cross Sections for Rotational Excitation of Hydrogen. *Chem. Phys. Lett.* **1977**, *50*, 320–323.
- (12) Billing, G. D. The Semiclassical Treatment of Molecular Roto/Vibrational Energy Transfer. *Comput. Phys. Rep.* **1984**, *1*, 237–296.
- (13) Billing, G. D. *The Quantum-Classical Theory*; Oxford University Press: New York, 2002.
- (14) Semenov, A.; Babikov, D. Mixed Quantum/Classical Theory of Rotationally and Vibrationally Inelastic Scattering in Space-Fixed and Body-Fixed Reference Frames. *J. Chem. Phys.* **2013**, *139*, 174108/1–174108/14.
- (15) Loreau, J.; Zhang, P.; Dalgarno, A. Elastic Scattering and Rotational Excitation of Nitrogen Molecules by Sodium Atoms. *J. Chem. Phys.* **2011**, *135*, 174301/1–174301/8.
- (16) Semenov, A.; Ivanov, M. V.; Babikov, D. Ro-Vibrational Quenching of CO ( $\nu = 1$ ) by He Impact in a Broad Range of Temperatures: A Benchmark Study Using Mixed Quantum/Classical Inelastic Scattering Theory. *J. Chem. Phys.* **2013**, *139*, 074306/1–074306/11.
- (17) Bowman, J. M.; Park, S. C. Quasiclassical Trajectory Studies of Rigid Rotor-Rigid Surface Scattering. I. Flat Surface. *J. Chem. Phys.* **1982**, *77*, 5441–5449.